It is clear that modeling plays a key roll in determining appropriate loading methods for a determination of aircraft survivability. The proposed methodology uses dynamic finite element techniques to determine the dynamic response of selected aircraft undergoing an in-flight change of stiffness. Results of the dynamic analysis provide a pathway to the test engineer for determining the most appropriate test method. That method could either be static, dynamic, or a combination of the two (Fig. 10).

The team is currently investigating possible pneumatic, hydraulic, or combined loading techniques that could be used to apply dynamic loads during ground tests. It is anticipated that experimental ground testing can be applied for cases similar to case 1. The simulations have shown that the dynamic response and flutter resistance based on cases similar to that of case 2 result in deflections that, if applied to an actual wing, would lead to structural failure. Therefore, when flutter plays a key role in the dynamic response of the wing due to damage (case 2), it is anticipated that computational analyses will be used as the primary tool for accurately assessing postdamage survivability. Furthermore, it is important to note that a full structural evaluation should account for more than just a maximum yield stress criterion as was done here. Many other failure mechanisms from plasticity to cracking must also be considered.

References

[1]Maskew, B., "Program VSAERO Theory Document," NASA CR-4023, 1987.

[2]Negaard, G. R., "Finite Element Analysis of Ballistic Tests," U.S. Air Force Wright Aeronautical Lab., AFWAL-TR-88-3041, Wright–Patterson AFB, OH, 1988.

A. Palazotto
Associate Editor

Sound Waveform Effect on Disturbance Generation in Turbulent Jets at Aeroacoustic Interaction

V. G. Pimshtein*
Central Aerohydrodynamic Institute,
107005, Moscow, Russia

Introduction

AMONG a large number of the papers devoted to sound interaction with turbulent jets, the works associated with investigations of the spectral composition of the acoustic excitation affecting the disturbance generation and development in jets, aerodynamic jet parameters, and noise radiation occupy a significant place.[1] Usually the effect of different spectra of the acoustic excitation is considered in such works, particularly the effect of separate spectral components on the aeroacoustic interaction process, mainly on the process of vortex coupling, if the case in point is subsonic jets. As a rule in such cases, the important role of the fundamental tone subharmonic, as the component affecting this process and resulting from it, is emphasized. Though it is known that the excitation spectrum and the process time dependency should cause one another, the effect of the sound waveform itself on the process of aeroacoustic interaction usually is not taken into account. Sokolov et al.[2] presented some evidence that the form of the sound wave can substantially affect the coherent structure initiation, and Vlasov et al.[3] studied the sound waveform effect on low-speed (up to 20 m/s) jet spreading. However, the average aerodynamic characteristics, which do not allow for a definition of details of the aeroacoustic interaction mechanism, were measured in these works.

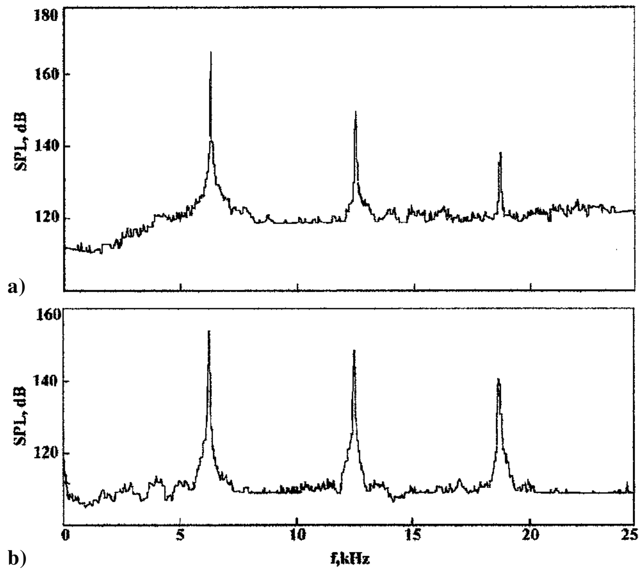

Fig. 1 Sound pressure spectra at different distances from the HG in frequency bands Δf = 32 Hz, f = 6.3 kHz: —l = a) 5 and b) 150 mm.

The purpose of this Note is to investigate the sound waveform effect on coherent structure generation in subsonic and supersonic turbulent jets under lateral high-intensity excitation by sinusoidal and sawtoothlike waves.

The experiments were carried out in a large anechoic chamber of the Acoustic Division of the Central Aerohydrodynamic Institute with unheated subsonic ($\bar{p}_o = 1.4$) and underexpanded supersonic air jets issuing from convergent nozzle ($M = 1.0$, $\bar{p}_o = 3.4$–3.7) and a supersonic jet issuing from the convergent–divergent nozzle ($M = 2.0$, $\bar{p}_o = 6.2$) with exit diameter $d = 20$ mm. (Here $\bar{p}_o = p_o/p_a$ is the pressure ratio at the nozzle, p_o is the total pressure in the settling chamber of the nozzle, p_a is the ambient pressure, and M is the nozzle design Mach number.) Hartman generators (HGs) with a frequency of 4.0–8.5 kHz were used as the sound sources. The sinusoidal high-intensity sound wave near the generator becomes enriched with higher harmonics during its propagation and is transformed into a sawtoothlike wave. This circumstance was used in the experiments: Fig. 1 presents sound pressure spectra at different distances from the generator. Acoustic measurements (rms value of the sound pressure) were carried out with a Bruel and Kjaer microphone (model 4136) located near the nozzle edge and a Bruel and Kjaer spectrometer (model 2032), where the accuracy of the data obtained is ± 1 dB. At small distances from the sound source ($l = 5$–10 mm) the sound wave is almost sinusoidal: the fundamental tone level exceeds the first harmonic by 15–20 dB (Fig. 1a). At large distances (100–150 mm) the difference between the levels of the fundamental and highest harmonics decreases (Fig. 1b) and the sinusoidal wave transforms into a sawtoothlike one. The sound pressure level (SPL) at the nozzle lip with sinusoidal excitation was 165 dB and for excitation by a sawtoothlike sound wave it was 155–170 dB. An SPL of 170 dB was achieved using sound reflectors. Visualization of jets, coherent structures, and sound waves was carried out with a direct shadowgraph technique with a spark source (the size of a luminous body of 0.8 mm and exposure time 2×10^{-7} s). It should be noted, however, that because the direct shadowgraph technique used is the most sensitive to the second derivative of intensity, sinusoidal sound waves cannot be seen in shadow pictures even at rather high sound intensity.

Results and Discussion

Figure 2 presents typical photographs of the subsonic jet ($\bar{p}_o = 1.4$) excited by a sinusoidal high-intensity sound wave (Fig. 2a; $f = 4.0$ kHz, SPL $= 165$ dB), by a sawtoothlike sound

Received 29 April 2002; revision received 15 May 2003; accepted for publication 20 May 2003.

*Senior Research Scientist, Acoustic Division, 17 Radio Str.

a)

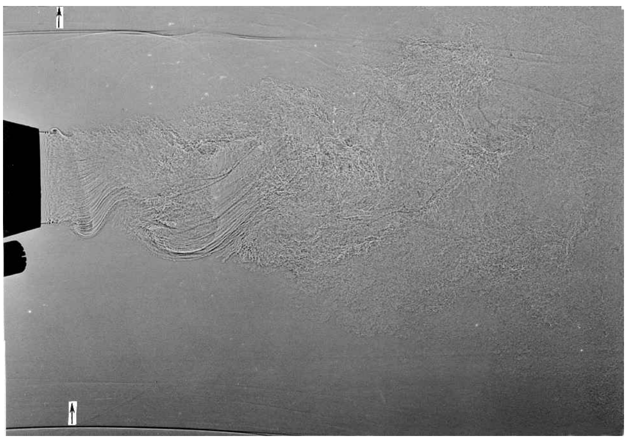

b)

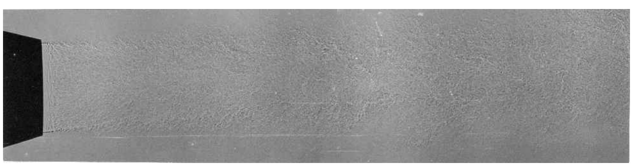

c)

Fig. 2 Subsonic jet ($\bar{p}_o$ = 1.4): a) under sinusoidal excitation, SPL = 165 dB, f = 4.0 kHz; b) under sawtoothlike sound wave excitation, SPL = 160 dB, f = 4.0 kHz; and c) an undisturbed jet.

wave (Fig. 2b; $f = 4.0$ kHz, SPL $= 160$ dB), and of the undisturbed jet (Fig. 2c). It is impossible to associate disturbance generation with some definite sound wave phase at sinusoidal excitation. Evidently the disturbance appears practically in-phase over the whole nozzle exit. The disturbance generated under sinusoidal excitation has no clear boundaries and this shows that aeroacoustic interaction occurs over a rather extended space-time interval.

Under excitation by a sawtoothlike wave the disturbance arises at the nozzle edge when the zone of maximum sound wave passes. Aeroacoustic interaction occurs in an extremely narrow space-time interval, and the disturbance has clear boundaries and is characterized by the presence of microstructure–longitudinal vortices (Görtler–Taylor vortices). Their scale is of boundary-layer-thickness order. At the considered lateral acoustic excitation the initiated disturbance is of the oblique vortex type. Its incidence depends on the jet velocity and the sound incidence angle.

The high-intensity acoustic excitation, close to the sinusoidal one, of the underexpanded supersonic jet issuing from a convergent nozzle at relatively small supercritical pressure ratios and characterized by a subsonic convective velocity causes lateral jet oscillations (Fig. 3a; $\bar{p}_o = 3.7$, $f = 4.0$ kHz, SPL $= 165$ dB). These oscillations are accompanied by sound radiation at the frequency of external excitation and seem to be associated with a supersonic lateral velocity of oscillation (Fig. 3a). The arrow shows the radiated sound wave.

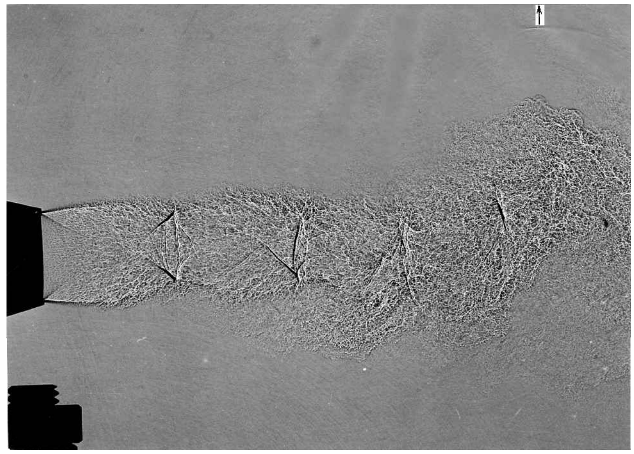

a)

b)

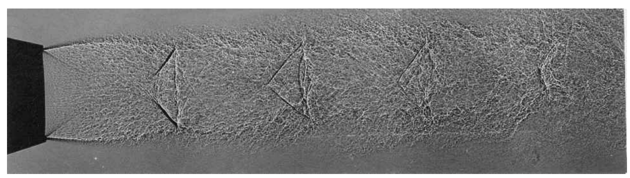

c)

Fig. 3 Supersonic jet issuing from a convergent nozzle ($\bar{p}_o$ = 3.7): a) under sinusoidal excitation, SPL = 165 dB, f = 4.0 kHz; b) under sawtoothlike sound wave excitation, SPL = 160 dB, f = 4.0 kHz; and c) an undisturbed jet.

In this case the periodic shock-wave formation in the jet undergoes no significant changes.

If such a supersonic jet is excited in the lateral direction by a sawtoothlike sound wave (Fig. 3b; $\bar{p}_o = 3.7$, $f = 4.0$ kHz, SPL $= 160$ dB), the distinct disturbances are generated at the nozzle lip, when the zone of maximum sound wave compression passes, similarly to the subsonic jet case. The periodic shock-wave formation in the jet can be disrupted. The microstructure of the generated disturbance is also characterized by Görtler–Taylor vortex presence. The shadowgraph of the undisturbed jet is presented in Fig. 3c. Lateral (or helical) jet oscillations under sinusoidal excitation are seen in Fig. 4 ($\bar{p}_o = 3.7$, $f = 4.0$ kHz, SPL $= 165$ dB), where the jet is shown at two different positions.

Owing to specificity of the tests conducted, when the sawtoothlikeness of the sound wave was achieved at the expense of a greater distance between the sound source and the jet, the rms value of SPL in the sawtoothlike sound wave was less than the SPL in the sinusoidal wave by 5–7 dB at the fundamental tone frequency. This fact, however, as the tests have shown, does not preclude revealing substantial distinctions of the coherent structures generated.

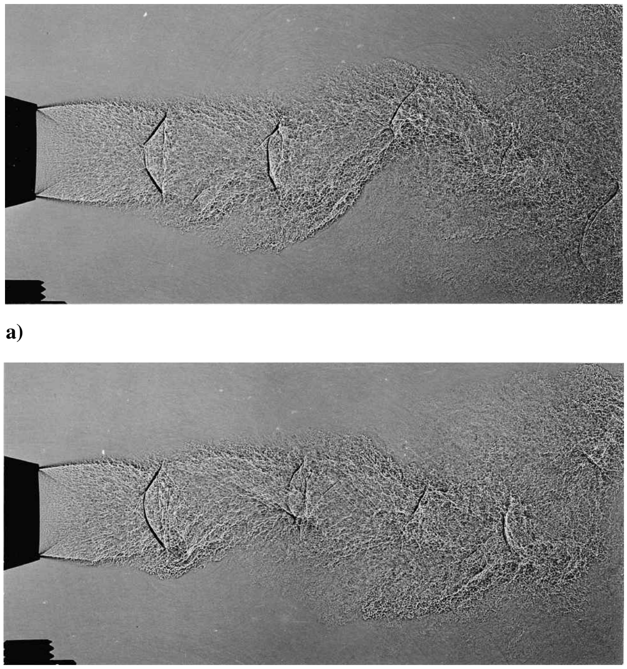

a) b)

Fig. 4 Supersonic jet oscillations under sinusoidal excitation ($\bar{p}_o$ = 3.7, SPL = 160 dB, f = 4.0 kHz).

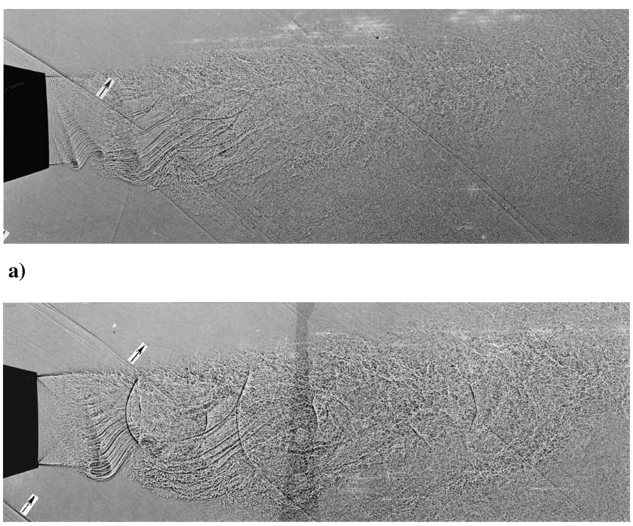

a) b)

Fig. 5 Jets under sawtoothlike sound wave excitation (SPL = 165 dB, f = 8.5 kHz, sound incidence angle = 60 deg): a) subsonic ($\bar{p}_o$ = 1.4) and b) supersonic ($\bar{p}_o$ = 3.4).

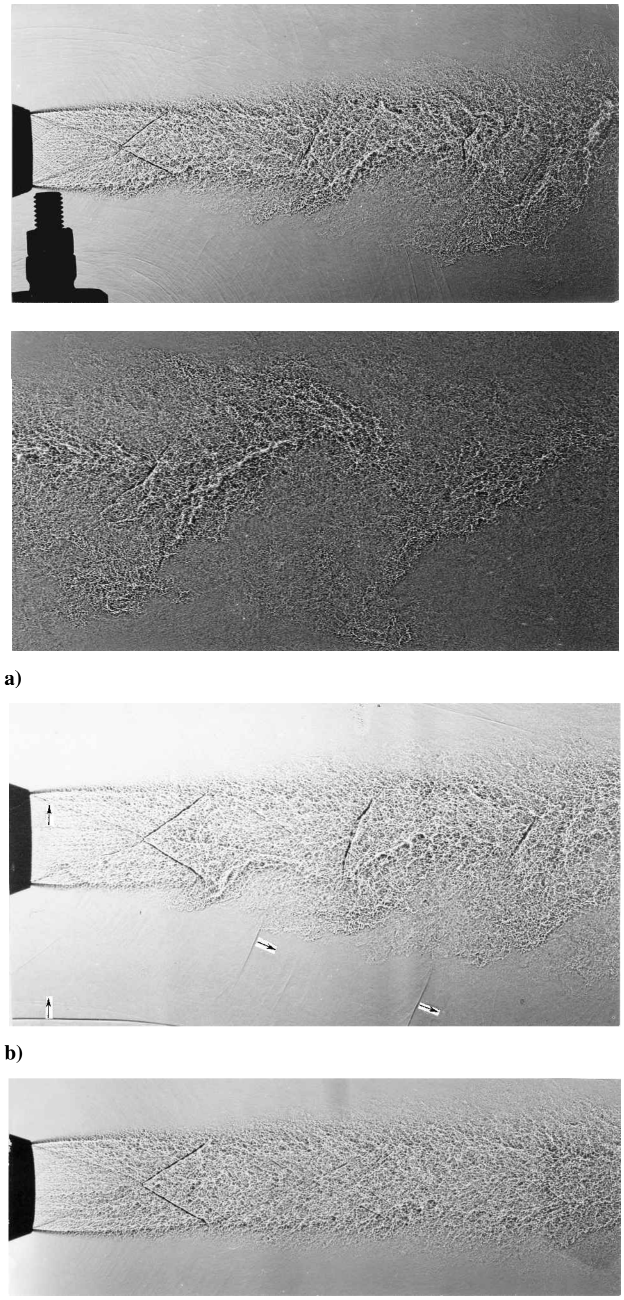

a) b) c)

Fig. 6 Supersonic jet issuing from a supersonic nozzle (M = 2.0, $\bar{p}_o$ = 6.2): a) under sinusoidal excitation, SPL = 162 dB, f = 8.5 kHz; b) under sawtoothlike sound wave excitation, SPL = 156 dB, f = 8.5 kHz; and c) an undisturbed jet.

If the SPL in the sawtoothlike sound wave increased up to the value obtained under sinusoidal excitation that was achieved using the sound parabolic reflector, the disturbances and their microstructure were expressed more clearly (Fig. 5; conditions at which this experiment was carried out are a little different from the aforementioned conditions).

Under sinusoidal excitation of the supersonic jet issuing from a convergent–divergent nozzle at moderate values of pressure ratio in the nozzle ($M = 2.0$, $\bar{p}_o = 6.2$) characterized by supersonic convective velocity, a coherent structure appears in the jet. Its scale depends on jet excitation frequency and velocity and the structure extends over a considerable distance, in the case considered, over the distance exceeding $20d$ (Fig. 6a; $f = 8.5$ kHz, SPL = 162 dB). The jet does not oscillate laterally, and its expansion is the result of the disturbance dimensions increasing with their motion along the irradiated jet boundary.

If the supersonic jet with supersonic convective velocity is excited by a sawtoothlike sound wave, disturbances with the space scales depending on the jet velocity and frequency appear. These disturbances move along the excited jet boundary, increasing in size, and radiate Mach waves into the ambient space at the external excitation frequency (Fig. 6b; $f = 8.5$ kHz, SPL = 156 dB). Figure 6c shows the undisturbed jet. The unsteady shock-wave pattern in the excited supersonic jet can arise and it may be associated with large-scale disturbances streamlined by a flow in its relative motion.[4] The tests carried out have shown that in this case the jet does not oscillate laterally at harmonic excitation either. It should be noted that the coherent structures generated under sinusoidal excitation of such a jet also produce disturbances in the ambient medium while moving with supersonic convective velocity. It appears, however, that due to the aforementioned peculiarity of the applied visualization technique, they are not seen in shadowgraphs.

Conclusions

At turbulent jet excitation by high-intensity sound the sound wave form plays a substantial role not only in forming coherent structures in the jet but also in forming the jet structure itself. Sinusoidal excitation generates rather extended vortices in jets and can cause lateral jet oscillations. Sawtoothlike wave excitation leads to the formation of compact disturbances both in subsonic and supersonic jets. The intrinsic shock-wave formation of supersonic jets can be destroyed in this case and the disturbance movement along the jet boundary at supersonic convective velocity is accompanied by Mach wave radiation.

Acknowledgment

This work was supported by the Russian Fund of Fundamental Investigations (Grant 03-01-00492).

References

[1]Ginevsky, A. S., Vlasov, Y. V., and Karavosov, R. K., *Acoustic Control of Turbulent Jets,* Physmathlit, Moscow, 2001 (in Russian).

[2]Sokolov, M., Kleis, S. J., and Hussain, A. K. M. F., "Coherent Structures Induced by Two Simultaneous Sparks in Axisymmetric Jet," *AIAA Journal*, Vol. 19, No. 8, 1981, pp. 1000–1008.

[3]Vlasov, Ye. V., Ginevsky, A. S., Karavosov, R. K., and Makarenko, T. M., "Effect of Non-Harmonic Signal on Turbulent Jet," *Inzhenerno-Fizicheskii Zhurnal*, Vol. 74, No. 5, 2001, pp. 33–35 (in Russian).

[4]Pimshtein, V. G., "Disturbance Generation in Supersonic Jets Under Acoustic Excitation," *AIAA Journal*, Vol. 32, No. 7, 1994, pp. 1345–1349.

W. J. Devenport
Associate Editor

Optimal Disturbances in Boundary Layers Subject to Streamwise Pressure Gradient

Anatoli Tumin*
University of Arizona, Tucson, Arizona 85721
and
David E. Ashpis†
NASA John H. Glenn Research Center at Lewis Field, Cleveland, Ohio 44135

Introduction

LAMINAR–TURBULENT transition in shear flows is still an enigma in the area of fluid mechanics. The conventional explanation of the phenomenon is based on the instability of the shear flow with respect to infinitesimal disturbances. The conventional hydrodynamic stability theory deals with the analysis of normal modes that might be unstable. The latter circumstance is accompanied by an exponential growth of the disturbances that might lead to laminar–turbulent transition. Nevertheless, in many cases, the transition scenario bypasses the exponential growth stage associated with the normal modes. This type of transition is called *bypass transition.* An understanding of the phenomenon has eluded us to this day. One possibility is that bypass transition is associated with so-called algebraic (nonmodal) growth of disturbances in shear flows.[1,2]

A numerical analysis of spatial nonmodal growth within the scope of the linearized boundary-layer equations for an incompressible flow over a flat plate was carried out in Refs. 3 and 4. Spatial analysis within the scope of the linearized Navier–Stokes equations (quasi-parallel approximation of compressible and incompressible flows) was presented in Refs. 5–7. Recently, the method of Ref. 4 was generalized for the case of compressible boundary layers.[8] The main results of these theoretical models are as follows: 1) A system of counter-rotating streamwise vortices, which are periodic in the spanwise direction, provides the strongest growth of the disturbance. 2) There is an optimal spacing of the streamwise vortices, which leads to the strongest effect.

The effect of pressure gradients on the transient growth mechanism was considered within the scope of temporal theory by Corbett and Bottaro[9] and within the scope of spatial theory by Tumin and Reshotko.[7] Both studies were based on the quasi-parallel flow assumption. Tumin[10] analyzed the pressure-gradient effect for the Falkner–Skan profile within the scope of an analytical model when the spanwise wave number is very small. The pressure-gradient effect within the scope of spatial theory with nonparallel base flow and finite spanwise wave numbers has not yet been considered.

Another motivation for the present work stems from separation flow control on low-pressure turbines (LPTs). The performance of LPTs is strongly affected by the flow separation. There is a possibility of delaying the boundary-layer separation by tripping the boundary layer with the help of roughness elements or other devices. Usually, a trial-and-error method is used to determine an appropriate placement of the control elements. This approach is time consuming and expensive. A recent investigation by Reshotko and Tumin[11] demonstrated that roughness-induced transition might be related to the transient growth mechanism.

Periodically spaced in the spanwise direction, roughness elements generate a system of counter-rotating streamwise vortices. Due to a secondary instability mechanism, the streamwise vortices can lead to earlier transition to turbulence. They also provide a mixing enhancement due to redistribution of the streamwise momentum. Consequently, optimization of the streamwise vortices for maximum energy growth leads to maximization of the flow control effectiveness. In the present work, an analysis of the optimal disturbances/streamwise vortices associated with the transient growth mechanism is performed for boundary layers in the presence of a streamwise pressure gradient. The theory will provide the optimal spacing of the control elements in the spanwise direction and their placement in the streamwise direction.

Governing Equations

Because the flows of interest have relatively low Mach numbers, we consider steady three-dimensional disturbances in an incompressible two-dimensional boundary layer. We choose the streamwise coordinate x along the surface. The coordinate y will measure distance from the wall. We define a small parameter $\varepsilon = \sqrt{(\nu / U_{\text{ref}} L_{\text{ref}})}$ that is the inverse square root of the Reynolds number, and ν, U_{ref}, and L_{ref} are viscosity, reference velocity, and reference length, respectively. The streamwise coordinate is scaled with L_{ref} while the vertical coordinate y and spanwise coordinate z are scaled with $\sqrt{(\nu L_{\text{ref}} / U_{\text{ref}})}$. The following scaling is assumed for the velocity disturbances u, v, and w and the pressure p:

$$u \sim U_{\text{ref}}, \qquad v \sim \varepsilon U_{\text{ref}}, \qquad w \sim \varepsilon U_{\text{ref}}, \qquad p \sim \varepsilon^2 \rho U_{\text{ref}} \quad (1)$$

This scaling of the linearized Navier–Stokes equations and neglecting the curvature effects lead to the governing equations for Görtler instability, with the Görtler number equal to zero. We look for a periodic solution in the spanwise direction, with the corresponding wave number β. The governing equations for

Received 21 February 2003; presented as Paper 2003-4242 at the AIAA 33rd Fluid Dynamics Conference, Orlando, FL, 23–26 June 2003; revision received 1 August 2003; accepted for publication 4 August 2003.

*Associate Professor, Department of Aerospace and Mechanical Engineering; tumin@email.arizona.edu. Senior Member AIAA.

†Aerospace Engineer. Senior Member AIAA.